







Effect of relative humidity on hydrogen peroxide production in water droplets†

Maria T. Dulay¹ , Carlos Alberto Huerta-Aguilar¹ , Christian F. Chamberlayne¹ ,
Richard N. Zare^{1*} , Adriaan Davidse²  and Sinisa Vukovic³ 

¹Department of Chemistry, Stanford University, Stanford, CA 94305, USA; ²PO Box 93167 Healdton PO Burlington, ON L7M 4A3, Canada and ³MineRP, 333 Bay Street, Toronto, ON M5H 2T6, Canada

Research Article

†The original version of this article was published with an incorrect ORCID ID for an author. A notice detailing this has been published and the error rectified in the online PDF and HTML copies.

Cite this article: Dulay MT, Huerta-Aguilar CA, Chamberlayne CF, Zare RN, Davidse A, Vukovic S (2021). Effect of relative humidity on hydrogen peroxide production in water droplets. *QRB Discovery*, 2: e8, 1–6 <https://doi.org/10.1017/qrd.2021.6>

Received: 20 June 2021

Revised: 19 July 2021

Accepted: 21 July 2021

Key words:

H₂O₂ quantification; hydrogen peroxide; microdroplet chemistry; reactive oxygen species; relative humidity; respiratory viral infections

Author for correspondence:

*Richard N. Zare,

E-mail: zare@stanford.edu

Present address: Maria T. Dulay, Department of Radiology, Stanford School of Medicine, Stanford, CA 94305, USA

Present address: Carlos Alberto Huerta-Aguilar, School of Engineering and Sciences, Tecnológico de Monterrey, 5718 Atlixcáyotl, 72453 Puebla, Mexico

Maria T. Dulay and Carlos Alberto Huerta-Aguilar contributed equally to this work.

Abstract

Mist is generated by ultrasonic cavitation of water (Fisher Biograde, pH 5.5–6.5) at room temperature (20–25 °C) in open air with nearly constant temperature (22–25 °C) but varying relative humidity (RH; 24–52%) over the course of many months. Water droplets in the mist are initially about 7 μm in diameter at about 50% RH. They are collected, and the concentration of hydrogen peroxide (H₂O₂) is measured using commercial peroxide test strips and by bromothymol blue oxidation. The quantification method is based on the Fenton chemistry of dye degradation to determine the oxidation capacity of water samples that have been treated by ultrasonication. It is found that the hydrogen peroxide concentration varies nearly linearly with RH over the range studied, reaching a low of 2 parts per million (ppm) at 24% RH and a high of 6 ppm at 52% RH. Some possible public health implications concerning the transmission of respiratory viral infections are suggested for this threefold change in H₂O₂ concentration with RH.

Introduction

Interest in understanding the role of relative humidity (RH) in modulating the transmission and seasonality of infectious diseases has resulted in an increase in recent published studies (Han *et al.*, 2020; Lin and Marr, 2020; Moriyama *et al.*, 2020; Ma *et al.*, 2021). It has been known for decades that respiratory droplets in ambient air evaporate until they reach equilibrium. Because respiratory droplets are saturated (Walker and Wells, 1961) while ambient air typically is not, a vapour pressure gradient is produced between the droplet surface and the ambient air that is the driving force for evaporation, which has been shown to be influenced by RH (Marr *et al.*, 2019). The equilibrium size of a droplet, which is attained within a few seconds (Nicas and Jones, 2009; Shaman and Kohn, 2009; Halloran *et al.*, 2012) is dependent on RH (Marr *et al.*, 2019), and the size of the droplet determines its gravitational settling speed (Xie *et al.*, 2007; Božič and Kanduč, 2021). The changes in chemistry within these smaller droplet sizes have been proposed as a cause of influenza virus degradation. The stability of viruses may depend on chemical events such as osmotic bursting or changes in pH that may alter a protein's geometry (Marr *et al.*, 2019). Virus inactivation at the air–water interface of an aerosolized droplet has also been proposed although the mechanism is poorly understood (Božič and Kanduč, 2021).

Our own studies of water microdroplets offer insight into the chemistry that plays a role in the inactivation of pathogenic species. The chemical microenvironment of a water microdroplet involves the formation of reactive oxygen species (ROS), which includes the hydroxyl radical (•OH) and hydrogen peroxide (H₂O₂) because of the high electric field present at the air–water interface of a microdroplet (Lee *et al.*, 2019). Aqueous microdroplets of nominal 10-μm size have been shown to act as a bactericide in the inactivation of *Escherichia coli* and *Salmonella typhimurium* where the presence of ROS in microdroplets and the surface charge of microdroplets play roles in the destruction of these bacterial cells (Dulay *et al.*, 2020). In this study, the results show that the concentration of H₂O₂ in a water microdroplet has a linear relationship within a given range of RH that aligns with the seasonality of infectious diseases. It is suggested that understanding the role of RH in the formation of ROS will aid in designing methods to reduce or prevent the transmission of airborne infectious diseases.

Materials and methods

Chemicals and materials

Biograde water (Corning) was purchased from Fisher Scientific (Waltham, MA) and used without further purification. MQuant peroxide test strips for the colorimetric detection of H₂O₂ in the range of 0.5–25 ppm were purchased from Sigma-Aldrich (Milwaukee, WI) and

© The Author(s) 2021. Published by Cambridge University Press. This is an Open Access article, distributed under the terms of the Creative Commons Attribution-NonCommercial-ShareAlike licence (<http://creativecommons.org/licenses/by-nc-sa/4.0/>), which permits non-commercial re-use, distribution, and reproduction in any medium, provided the same Creative Commons licence is included and the original work is properly cited. The written permission of Cambridge University Press must be obtained for commercial re-use.

stored at 4 °C. Bromothymol blue (BTB) and iron (II) sulphate (ferrous sulphate, FeSO₄) were purchased from Sigma-Aldrich (Milwaukee, WI) and used as received.

A FITNATE ultrasonic mist maker was purchased from Amazon (Seattle, WA). This mist maker contained a 16 mm × 1.2 mm ceramic piezoelectric disc with a resonant frequency of 1.70 MHz and a resonant impedance of less than 1 Ω. The maximum spray volume was approximately 110 ml h⁻¹. Becton–Dickinson 96-well microplates, Becton–Dickinson plastic petri dishes, and 1.5-ml Eppendorf tubes were purchased from Fisher Scientific (Waltham, MA). RH and temperature were recorded using a HOBO UX100–011 data logger (Onset Computer Corporation, Bourne, MA).

Instruments

An Azure Biosystems (Dublin, CA) absorbance microplate reader (450 nm) was used to monitor the Fenton reaction/BTB chemical assay. A HELOS 2750 Particle Size Analyzer (Sympatec GmbH, Clausthal-Zellerfeld, Germany) was used to measure the size of the water droplets produced from the mist maker.

Mist generation and collection

The mist maker was positioned at 45° from the bottom of a 500-ml beaker filled with a total volume of 250–300 ml of Biograde water. The angle was chosen so that the waterspout from the mist maker hits the beaker wall at a height approximately 1.6 cm from the surface of the water to minimise water loss from the beaker during the mist generation and collection. The total volume of Biograde water in the beaker containing the mist maker was brought to 250 ml. Operation of the mist maker was done under ambient environmental conditions. Mist was collected within the first 5–10 min of operation as it condensed into a plastic petri dish that was placed next to the beaker. No additional water was added to the beaker during the mist collection as the volume of water loss was minimal. The condensed mist was placed into Eppendorf tubes and immediately analysed using a chemical assay. The temperature of the water in the beaker did not exceed 27°C as measured with a thermometer. The laboratory RH was measured using the RH sensor described above which was located near the experimental setup. Measurements were recorded over many months so that the variation with RH of the room could be determined. The local RH surrounding the droplets in the mist is expected to be higher from the droplets' evaporation and has not been measured. Nevertheless, it is expected to scale with the RH in the room.

H₂O₂ quantification

Test strip method

This semi-quantitative method involved the use of commercial MQuant H₂O₂ test strips. A test strip was placed for approximately 10 s into at least 50 µl of mist sample. Any colour change to blue was indicative of the presence of H₂O₂ and the shade of blue was compared to a colour chart on the test strip bottle. This test strip approach provided a rapid, but semi-quantitative measure of H₂O₂ concentration and was used primarily to confirm the presence of H₂O₂.

BTB chemical assay

This quantitative chemical assay is based on the Fenton reaction, with BTB as the OH radical scavenger. Stock solutions of 1.0 mM BTB and 5.0 mM ferrous sulphate (FeSO₄), were prepared in

Biograde water. For each sample analysis, 5 µl of BTB stock solution and 10 µl FeSO₄ stock solution were added to 200 µl of mist sample to be analysed. An additional 35 µl of Biograde water was added to the mixture to bring the total volume to 250 µl. A control solution was prepared by mixing 5 µl BTB stock solution and 245 µl Biograde water for a final total volume of 250 µl. The blank was 250 µl of Biograde water. The changes in absorbance were converted to concentration, using Beer's law where the molar absorptivity (ϵ) of BTB is 13,000 M⁻¹ cm⁻¹ at 450 nm. The second-order reaction rate was obtained by plotting 1/[BTB] as a function of time (s). The resulting slope was converted to apparent hydrogen peroxide concentration, [H₂O₂]_{app}, from a calibration curve prepared using H₂O₂ concentrations ranging from 0 to 50 mg l⁻¹. A calibration curve was prepared at the beginning of the experiments done on each day.

A volume of 250 µl of each calibration or test sample was added to a well in a 96-well plate. Absorbance measurements of each sample in each well were taken every 45 s at 450 nm for a total scan time of 25 min. To verify that oxidised BTB from a change in solution pH was not present during the reaction, the absorbance at 650 nm was monitored.

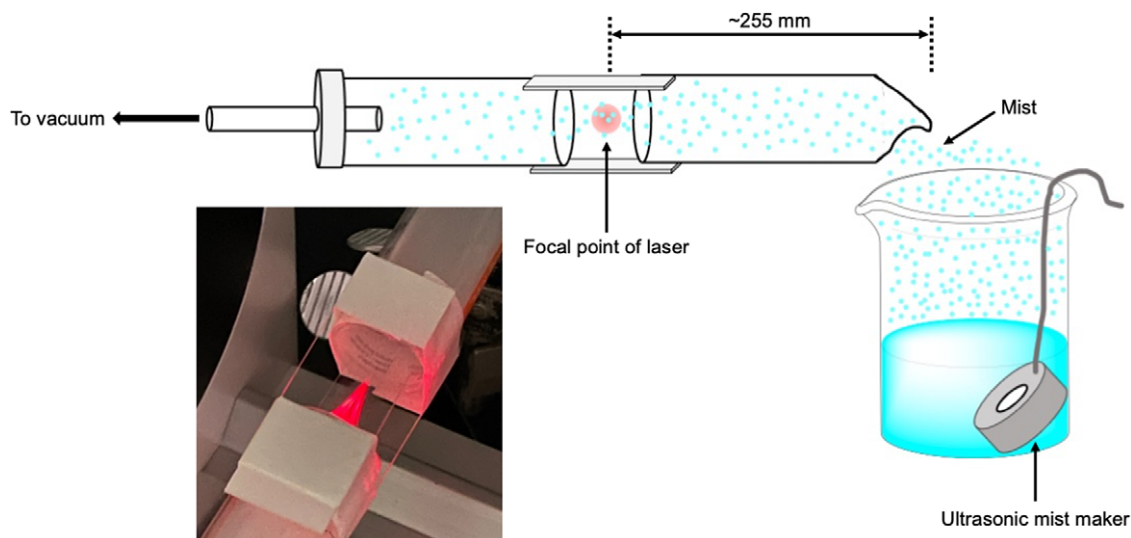
Mist droplet size measurement

To achieve a steady stream of mist flow to the focal point of the laser of the HELOS 2750 Particle Size Analyzer, the droplets in the mist were pulled into a tube attached to house vacuum. The tube was prepared by connecting 50-ml plastic Falcon tubes (30-mm i.d.) with two 25 mm × 75 mm glass slides positioned at the top and bottom of tubes arranged in series as shown in Scheme 1. The focal point of the laser was approximately 255 mm from the opening of the tube through which the mist entered. Two or four minutes after turning on the mist maker, size measurements were recorded for 1 s. The reference was taken at ambient conditions with the room light off in the absence of mist (mist maker off). The measurements were done in triplicate.

Results and discussion

The history of this experimental study might help to put our results and their limitations in better perspective. Once we understood that tiny water droplets could be used as a biocide (Dulay *et al.*, 2020) we turned our attention to exploring what factors might lead to the production of higher concentrations of H₂O₂. We examined various grades of water, the water temperature, and the possible addition of different solutes, such as salt and carbon dioxide, that might affect the H₂O₂ concentration. This study went on for many months, during which time we noticed that the results obtained were variable. This variability was traced to the percentage RH in the surrounding air caused by seasonal changes in the laboratory air environment. The present results are incomplete and should be regarded as only a start of the question of how %RH affects the H₂O₂ concentration in water droplets found in a mist. Certainly, a better study in the future would be to control the %RH and to vary it under our control. In this way we might cover a wider range of %RH, which would be desirable. Nevertheless, the results were to us so striking that we want to share them in their present form.

The size of water droplets in the ultrasonically generated mist was characterised by light scattering, as described above. The size distribution data were fitted to a normal log function whose peak is defined as the droplet diameter. Fig. 1 shows that the droplet diameter in the mist is 6.71 µm ($n = 3$, RSD = 0) with an average



Scheme 1. Setup for droplet size measurements. The photo shows the laser light scattering off the droplets in the mist as they travelled through the tube while being suctioned under vacuum.

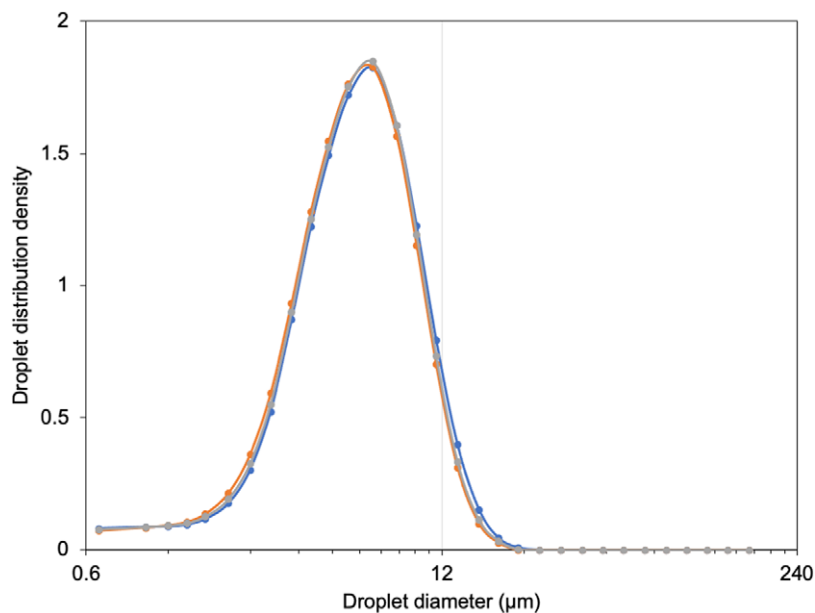


Fig. 1. Plot of droplet distribution density as a function of droplet diameter in mist generated by a mist maker immersed in approximately 300 ml Biograde water. Each plot represents 1 s of data acquisition: trial 1 (blue circles) with mist maker on for 2 min prior to measurement; trial 2 (orange circles) with mist maker on for 4 min prior to measurement; and trial 3 (grey circles) with mist maker on for 2 min prior to measurement. Trials 1 and 3 were acquired under identical conditions to test reproducibility.

distribution density of 1.83 ($n = 3$, RSD = 0.70%). Droplet diameters ranged in size from 1 to 19.4 μm with a droplet distribution density of 0.081 and 0.044, respectively. Based on previous studies on the production of hydrogen peroxide in droplets formed by spraying water (Lee *et al.*, 2019) and condensing water vapour (Lee *et al.*, 2020), these droplet sizes are expected to produce readily detectable concentrations of H_2O_2 .

The concentration of H_2O_2 present in the mist generated was determined using Fenton chemistry with BTB as the dye indicator. Fenton chemistry is rather complex and has been summarised elsewhere (Babuponnusami and Muthukumar, 2014). A pseudo-second-order dependence on the disappearance of the BTB concentration is observed at long time (Fig. 2a). Its pseudo-second-order rate constant is observed to have a linear dependence on the initial

H_2O_2 concentration (Fig. 2b). While Fig. 2 only shows 0.1–8 ppm, this linear dependence was verified for the range of 0.1–150 ppm ($R^2 = 0.997$). A calibration curve for determining the H_2O_2 initial concentration was constructed from the pseudo-second-order rate constant in BTB. Hydrogen peroxide test strips were used to confirm the presence of H_2O_2 in the mist samples.

From the assay, the concentration of H_2O_2 present in mist was measured at different values of the RH percentage (%RH) in the laboratory. Fig. 3 shows the relationship between $[\text{H}_2\text{O}_2]$ and %RH. As the %RH increases between the range of 24 and 52%, at 25°C, the concentration of H_2O_2 increases linearly. These results might be compared to what has been reported for the H_2O_2 concentration in droplets formed from condensed water vapour on a cold substrate (Lee *et al.*, 2020). It was found that at 0.5 min, the average

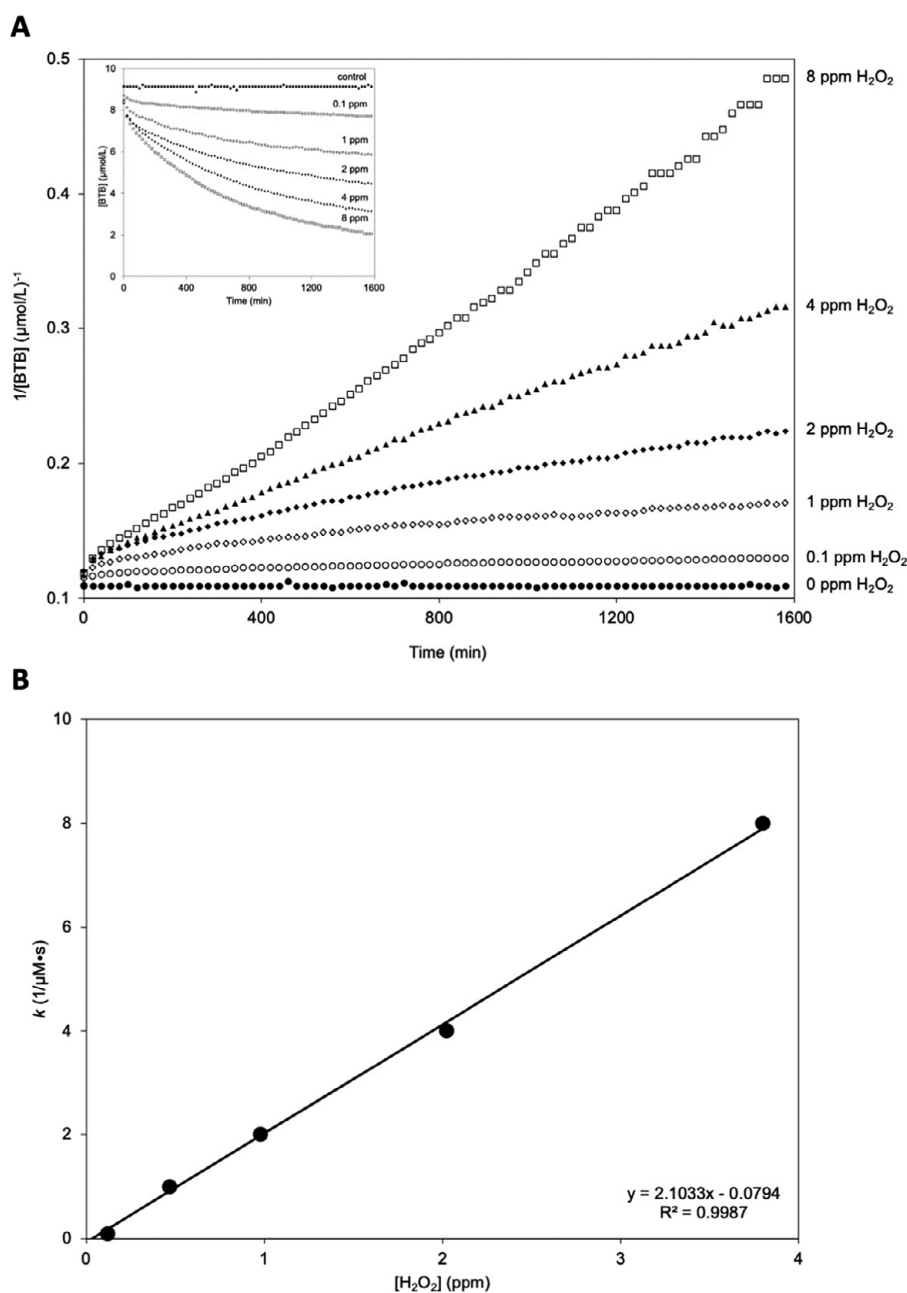


Fig. 2. (a) Plot of time versus $1/[\text{BTB}]$ for 0–8 ppm H_2O_2 . (b) Calibration curve created by plotting the rate constant k as a function of $[\text{H}_2\text{O}_2]$.

microdroplet diameter was $4.0 \pm 2.7 \mu\text{m}$, and the H_2O_2 production yield was less than 1.0 ppm. Under continuous cooling, the microdroplet diameter increased to an average value of $7.7 \pm 5.7 \mu\text{m}$ after 2 min. The H_2O_2 production yield reached a maximum value of ~ 3.9 ppm at 2 min. After 5 min, microdroplets continued to grow with an average diameter of $12.5 \mu\text{m}$. At this time point, droplets with diameters of $\sim 100 \mu\text{m}$ or larger were formed and the concentration of H_2O_2 dropped below the level of detection, being so diluted by the added amount of condensed water. Unfortunately, the %RH was not recorded in this earlier study, so it is difficult to make the comparison quantitative. It is possible that the higher hydrogen peroxide concentration reported in this study arises in part from ultrasonic cavitation used in our mist maker, which is known to produce radicals (Riesz *et al.*, 1985) although as will be

explained in what follows, this cannot explain the variation of H_2O_2 concentration with %RH.

The mechanism for H_2O_2 generation in aqueous microdroplets surrounded by a hydrophobic medium is presently not completely understood. We know that H_2O_2 formation occurs rapidly in less than a millisecond as demonstrated by chemical trapping of H_2O_2 reaction products in a spray in air entering a mass spectrometer (Gao *et al.*, 2019). Microdroplets are known to have a strong electric field at the interface and an internal electric double layer (EDL) (Chamberlayne and Zare, 2020; Xiong *et al.*, 2020). A leading theory for H_2O_2 production is that it arises from the recombination of hydroxyl radicals at the air–water interface, which is promoted by this special environment (Lee *et al.*, 2019). The hydroxyl radicals are thought to originate from hydroxide anions that lose an electron

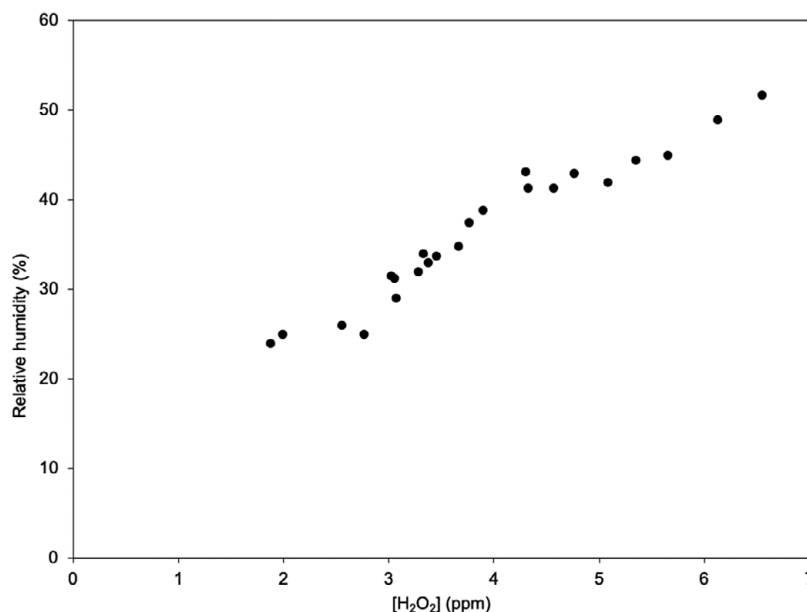


Fig. 3. A plot of H₂O₂ concentration as a function of %RH in the laboratory during the generation of mist using Biograde water. Each point represents a single measurement.

promoted by the strong electric field from the EDL (Lee *et al.*, 2019). There appears to be a steady-state amount of H₂O₂ formed which depends on the radius of the droplet. Again, the mechanism behind this has not been established. The nearly linear variation of the H₂O₂ concentration with %RH, evident in Fig. 3, might offer a clue to advancing our understanding of this phenomenon.

All droplets formed from the mist maker are believed to start with the same H₂O₂ concentration but then undergo evaporation at different rates depending on the RH. The rate of evaporation depends on many factors and has been reviewed elsewhere (Božič and Kanduč, 2021). H₂O₂ becomes increasingly concentrated in the remaining water droplet (Hultman *et al.*, 2007). If evaporation were the only mechanism, then it would be expected that the H₂O₂ would accumulate in the evaporating droplets, such that the H₂O₂ concentration would increase as the RH is lowered for which evaporation proceeds more rapidly. But this would lead to exactly the opposite trend to what is observed in Fig. 3. This indicates that whatever mechanism is responsible for the H₂O₂ formation also has a loss mechanism that establishes a radius-dependent steady-state condition for the H₂O₂ amount. This loss mechanism might be a combination of decomposition of H₂O₂ and evaporation of the entire droplet. Further support for this loss mechanism comes from our observation that when the temperature of the Biograde water was raised, the production of H₂O₂ in the collected droplets decreased.

In understanding our observations, it is important to realise that these experiments are not done with an isolated droplet but rather in a mist of droplets. If one creates mist, many of the nanosized droplets constituting mist will aggregate into micron-sized water droplets (and then condense for our measurements). On the other hand, if one injects microdroplets into vacuum many droplets will evaporate to nanodroplets. Evaporation rates and evaporation rate constants (related to surface tension) depend on the droplet sizes. But so do the aggregation rates which also depend on the amounts of droplets. Mist and droplets exist in a dynamic equilibrium, where some mist is turning into droplets and some droplets disintegrating into mist. The %RH in the mist is expected to be much higher than the %RH in the surrounding air. However, the formation and

steady-state behaviour of the mist depend on the rate of evaporation, and therefore the %RH of the surrounding air affects the resulting H₂O₂ concentration.

We know that at the extremes of small water clusters and very large water droplets, there is no detectable presence of H₂O₂. This reasoning suggests that we are observing a ‘Goldilocks effect’ in which droplets that are too large or too small have diminished H₂O₂ concentration compared to intermediate sizes. Let us consider how the optimal balance between these two extremes might occur. The falloff in H₂O₂ concentration as the size of the water droplet increases is relatively easy to explain. The reduction in surface area compared to volume washes out any surface area dependent effects. The falloff in H₂O₂ concentration as the size of the water droplet decreases is less intuitive. We suggest it is coming from interplay with the EDL inside the microdroplet. As the droplet size shrinks beyond some limit, the hydrogen peroxide generating mechanism is turned off and the loss mechanism becomes dominant. There exists a transition from nanoscale droplets, wherein the EDL of the nanodroplet from opposite sides of the droplet fully overlap, to larger droplets wherein the EDL is at the surface with a separate interior bulk solution to the microdroplet. This may help explain the Goldilocks effect observed. While we do not fully understand the mechanism, it possibly involves the interfacial solvation energy of the surface. The use of such energy in a mechanism could easily necessitate the existence of a bulk region in contact with a surface region and thus be prevented from existing in nanoscale droplets.

Fig. 3 also shows a remarkable increase by about a factor of three in the H₂O₂ concentration as %RH increases from 24 to 52%. Previous work (Dulay *et al.*, 2020) have clearly demonstrated that the ROS in sprayed water droplets (which we call aquaROS) are able to punch holes in the membranes of some bacteria causing them to be no longer viable. Preliminary results we have obtained on tobacco mosaic virus also show the killing power of aquaROS. Thus, we hypothesise that the water droplets at the high end of the percentage RH that we studied would also be a more potent bactericide and virucide. This conjecture is consistent with the observations presented elsewhere that viruses are effectively killed in small water droplets when the RH is in the range of 40–60% but

survive much better when the RH is less than 40% or greater than 60% (Birks and Rowlen, 2020; Lin and Marr, 2020; Božič and Kanduč, 2021). Although not without some controversy (Greenhalgh et al., 2021; Heneghan et al., 2021; Niazi et al., 2021), it does seem well established that viral respiratory diseases are primarily transmitted by airborne droplets. A number of public health consequences have been suggested (Davidse and Vukovic, 2020; Courtney and Bax, 2021). The results of the present study might provide a chemical basis for why maintaining %RH between 40 and 60% promotes human health.

Acknowledgements. C.A.H-A. would like to thank CONACyT for a post-doctoral fellowship. This work was supported by a SPARK Program in Translational Research at Stanford grant (Title: Spontaneously Formed Reactive Oxygen Species from Water for Pathogen Disinfection) and the US Air Force Office of Scientific Research through Basic Research Initiative grant (No. AFOSR FA9550-12-1-0400).

Author contributions. R.N.Z., M.T.D., C.A.H-A. and C.F.C. conceived the study. R.N.Z., M.T.D., C.A.H.A., C.F.C., A.D., and S.V. interpreted the experimental results. M.T.D. and C.A.H-A. performed the H₂O₂ quantitation experiments. M.T.D. and C.F.C. performed the droplet size measurements. All authors wrote the manuscript.

Conflicts of interest. The authors declare no conflicts of interest.

Open Peer Review. To view the open peer review materials for this article, please visit <http://dx.doi.org/10.1017/qrd.2021.6>.

References

- Babuponnusami A and Muthukumar K (2014) *A review on Fenton and improvements to the Fenton process for wastewater treatment*. Journal of Environmental Chemical Engineering **2**, 557–572.
- Birks JW and Rowlen KL (2020) Maintaining Classroom Humidity at 40–60% RH Would Reduce Transmission of Respiratory Viruses, Preprint September 2020. Available at <https://www.researchgate.net/lab/John-W-Birks-Lab>.
- Božič A and Kanduč M (2021) *Relative humidity in droplet and airborne transmission of disease*. Journal of Biological Physics **47**, 1–29.
- Chamberlayne CF and Zare RN (2020) *Simple model for the electric field and spatial distribution of ions in a microdroplet*. The Journal of Chemical Physics **152**, 184702.
- Courtney JM and Bax A (2021) *Hydrating the respiratory tract: An alternative explanation why masks lower severity of COVID-19*. Biophysical Journal **120**, 994–1000.
- Davidse A and Vukovic S (2020) Letter: Ex Vivo Amplification of Immune Response - Mechanism of Virucide within Exhaled Droplets of Infected Host. Preprint December 2020. <http://dx.doi.org/10.13140/RG.2.2.32536.83204>
- Dulay MT, Lee JK, Mody AC, Narasimhan R, Monack DM and Zare RN (2020) *Spraying small water droplets acts as a bacteriocide*. QRB Discovery **1**(e3), 1–8.
- Gao D, Jin F, Lee JK and Zare RN (2019) *Aqueous microdroplets containing only ketones or aldehydes undergo Dakin and Baeyer–Villiger reactions*. Chemical Science **10**, 10974–10978.
- Greenhalgh T, Jimenez JL, Prather KA, Tufekci Z, Fisman D and Schooley R (2021) *Ten scientific reasons in support of airborne transmission of SARS-CoV-2*. Lancet **397**, 1603–1605.
- Halloran SK, Wexler AS and Ristenpart WD (2012) *A comprehensive breath plume model for disease transmission via expiratory aerosols*. PLoS One **7**, e7088.
- Han L, Ran J, Chan K-H, Mak Y-M, Suen L, Cowling BJ and Yang L (2020) *Indoor environmental factors and acute respiratory illness in a prospective cohort of community-dwelling older adults*. The Journal of Infectious Diseases **222**, 967–978.
- Heneghan C, Spencer E, Brassey J, Plüddemann A, Onakpoya IJ, Evans DH, Only JM and Jefferson T (2021) *SARS-CoV-2 and the role of airborne transmission: A systematic review*. F1000Research **10**, 232. <https://doi.org/10.12688/f1000research.52091.1>
- Hultman C, Hill A and McDonnell G (2007) *The physical chemistry of decontamination with gaseous hydrogen peroxide*. Pharmaceutical Engineering **27**, 22–32.
- Lee JK, Han HS, Chaikasetin S, Marron DP, Waymouth RM, Prinz FB and Zare RN (2020) *Condensing water vapor to droplets generates hydrogen peroxide*. PNAS **117**, 30934–30941.
- Lee JK, Walker KL, Han HS, Kang J, Prinz FB, Waymouth RM, Nam HG and Zare RN (2019) *Spontaneous generation of hydrogen peroxide from aqueous microdroplets*. PNAS **116**, 19294–19298.
- Lin K and Marr LC (2020) *Humidity-dependent decay of viruses, but not bacteria, in aerosols and droplets follows disinfection kinetics*. Environmental Science & Technology **54**, 1024–1032.
- Ma Y, Pei S, Shaman J, Dubrow R and Chen K (2021) *Role of meteorological factors in the transmission of SARS-CoV-2 in the United States*. Nature Communications **12**, 3602.
- Marr LC, Tang JW, Van Mullekom J and Lakdawala SS (2019) *Mechanistic insights into the effect of humidity on airborne influenza virus survival, transmission, and incidence*. Journal of the Royal Society Interface **16**, 20180298.
- Moriyama M, Hugentobler WJ and Iwasaki A (2020) *Seasonality of respiratory viral infections*. Annual Review of Virology **7**, 2.1–2.19.
- Niazi S, Growth R, Spann K and Johnson GR (2021) *The role of respiratory droplet physicochemistry in limiting and promoting the airborne transmission of human coronaviruses: A critical review*. Environmental Pollution **276**, 115767.
- Nicas M and Jones RM (2009) *Relative contributions of four exposure pathways to influenza infection risk*. Risk Analysis **29**, 1291–1303.
- Riesz P, Berdahl D and Christman CL (1985) *Free radical generation by ultrasound in aqueous and nonaqueous solutions*. Environmental Health Perspectives **64**, 233–252.
- Shaman J and Kohn M (2009) *Absolute humidity modulates influenza survival, transmission, and seasonality*. PNAS **106**, 3243–3248.
- Walker JEC and Wells RE (1961) *Heat and water exchange in the respiratory tract*. The American Journal of Medicine **30**, 259–267.
- Xie X, Ho PL, Li Y, Chwang ATY and Seto WH (2007) *How far droplets can move in indoor environments – Revisiting the Wells evaporation–falling curve*. Indoor Air **17**, 211–225.
- Xiong H, Lee JK, Zare RN and Min W (2020) *Strong electric field observed at the interface of aqueous microdroplets*. Journal of Physical Chemistry Letters **11**, 7423–7428.